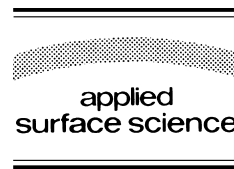




ELSEVIER

Applied Surface Science 130–132 (1998) 694–703



Electron emission properties of crystalline diamond and III-nitride surfaces

R.J. Nemanich^{*}, P.K. Baumann, M.C. Benjamin, O.-H. Nam, A.T. Sowers,
B.L. Ward, H. Ade, R.F. Davis

Department of Physics and Department of Materials Science and Engineering, North Carolina State University, Raleigh, NC 27695-8202, USA

Received 28 October 1997; accepted 20 December 1997

Abstract

Wide bandgap semiconductors have the possibility of exhibiting a negative electron affinity (NEA) meaning that electrons in the conduction band are not bound by the surface. The surface conditions are shown to be of critical importance in obtaining a negative electron affinity. UV-photoelectron spectroscopy can be used to distinguish and explore the effect. Surface terminations of molecular adsorbates and metals are shown to induce an NEA on diamond. Furthermore, a NEA has been established for epitaxial AlN and AlGa_N on 6H-SiC. Field emission measurements from flat surfaces of p-type diamond and AlN are similar, but it is shown that the mechanisms may be quite different. The measurements support the recent suggestions that field emission from p-type diamond originates from the valence band while for AlN on SiC, the field emission results indicate emission from the AlN conduction band. We also report PEEM (photo-electron emission microscopy) and FEEM (field electron emission microscopy) images of an array of nitride emitters. © 1998 Elsevier Science B.V. All rights reserved.

Keywords: Electron emission; Crystalline diamond; III-nitride

1. Introduction

The potential of cold cathode emission from diamond was recognized after initial photoemission and photo-threshold measurements of p-type natural diamond crystals [1,2]. These measurements involved UV light to measure the spectrum of photoelectron energies and the photo-electron yield vs. photon

energy. The development of CVD diamond film growth processes further stimulated this field of research because of the potential of fabricating low cost, electron emission structures. More recently, other wide bandgap semiconductors such as BN, AlN and AlGa_N alloys have also shown properties indicating a potential for application as cathode emitters [3–5].

It is evident that most cold cathode emission applications could not rely on the presence of UV light to excite the electron emission. As field emission from metals has been, and continues to be, an important area of research, it has been suggested that

^{*} Corresponding author. Department of Physics, North Carolina State University, Raleigh, NC 27695-8202, USA. Tel.: +1-919-515-3225; fax: +1-919-515-7331; e-mail: robert_nemanich@ncsu.edu.

field emission from a semiconductor with a negative electron affinity could provide electrons without a barrier to emission. To date, this possibility has not been realized.

In photoemission, the electrons are excited into the conduction band levels near the surface. Electrons near the surface may be emitted directly into vacuum, and the spectrum will represent a convolution of the valence band and conduction band density of states. Most electrons, though, will be scattered and thermalize to the conduction band minimum. For a traditional semiconductor with a positive electron affinity, these electrons are bound in the semiconductor and will eventually recombine with the photo-excited holes. For a negative electron affinity surface, the electrons near the surface at the conduction band minimum can also be emitted into vacuum.

In essence, the field emission process from semiconductors is more complex than the photoemission process. One basic difference is that there may be an insufficient supply of electrons to the conduction band. In comparison to metals, the supply of electrons is not a problem for moderate emission currents. For the wide bandgap semiconductors of diamond and the group III-nitrides, successful n-type doping has proved to be an illusive property. Thus, field emission measurements may reflect aspects of (i) the supply of electrons to the semiconductor, (ii) the transport of electrons to the surface, and finally (iii) the emission from the surface.

In this study, we summarize recent results for methods to obtain a negative electron affinity of diamond, show that the III-nitrides are also potential materials for cold cathode emitter structures, and address the relationship of photoemission and field emission. The materials of this study will be confined to either single crystals or high quality epitaxial films on single crystal substrates. In this way, issues related to the microstructure of the film may be minimized. More specifically, the studies focus on the surfaces of type IIB p-type diamond crystals and epitaxial films of AlN, GaN and their alloys on 6H-SiC substrates. While diamond is a cubic material, the nitrides form in the hexagonal wurtzite structure but are still characterized with tetrahedral sp^3 type bonding. The Al-Ga-nitrides form a continuous solid solution with a band gap that ranges from 3.4 eV for GaN to 6.2 eV for AlN.

2. Experimental techniques

The technique of UV photoemission spectroscopy (UPS) has been employed to characterize the electron affinity of a surface. The UPS technique is often employed for measurement of the valence band and surface electronic states of semiconductors. Two aspects of a UPS spectrum may be used to indicate a negative electron affinity of the surface. The two effects are the appearance of a sharp peak at low kinetic energy, and an extension of the spectral range to lower energy [6]. The sharp feature will appear at the largest (negative) binding energy in typical presentations of UPS spectra. This feature is attributed to electrons thermalized to the conduction band minimum. For a positive electron affinity, these electrons would be bound in the sample.

In addition to the sharp feature that is often evident in the spectra of a NEA semiconductor, the width of the photoemission spectrum (W) can be related to the electron affinity (χ). The spectral width is obtained from a linear extrapolation of the emission onset edge to zero intensity at both the low kinetic energy cutoff and at the high kinetic energy end (reflecting the valence band maximum). The following relations apply for the two cases:

$$\begin{aligned} \chi &= h\nu - E_g - W \text{ for a positive electron affinity,} \\ 0 &= h\nu - E_g - W \text{ for a negative electron affinity} \end{aligned} \quad (1)$$

where E_g is the bandgap and $h\nu$ is the excitation energy. We stress that the photoemission measurements cannot be used to determine the energy position of the electron affinity for the NEA surface. Careful measurements of the width of the spectra are helpful in distinguishing whether the effect is direct emission of the electrons from conduction band states or whether excitons are involved in the emission process. The effects of excitons have recently been reported by Bandis and Pate [7].

In addition to measurement of the electron affinity, the position of the surface Fermi level can be obtained. For a grounded sample, the Fermi level of the sample will be the same as that of the metal holder. The Fermi level of the metal can easily be determined, and the energy difference of the valence band maximum and the metal Fermi level yields the

position of the surface Fermi level of the semiconductor. In some instances, charging or photovoltage effects will complicate the analysis. To avoid these affects, we have employed p-type diamond and thin nitride layers grown on n-type SiC. Charging was not observed in any samples. Photovoltage effects are more difficult to discern. For the thin metals on diamond, emission was observed at the Fermi level indicating no photovoltage band bending. For the nitride layers, films are effectively undoped and the n-type SiC substrates will preclude substantial effects. We note that neither charging or photovoltage affects will change the width of the photoemission spectrum, so the analysis of the electron affinity is less complicated.

The field emission measurements in this study were completed using a moving probe system. With this method, an anode is positioned above the sample and the I vs. V is measured. The anode is stepped toward the sample surface, and the measurement is repeated. The I – V curves may be fit to the Fowler–Nordheim (F–N) expression which has been derived for emission from metals [8]. The F–N expression is often written as follows:

$$I = k \left(\frac{\beta V}{d} \right)^2 \exp \left(\frac{-6530 \phi^{3/2}}{\beta V} \right) \quad (2)$$

where I is the current, V the applied voltage (in volts), d is the distance between the anode and the surface (in μm), k is a constant, ϕ is the barrier (in eV) and β is the field enhancement factor due to the surface curvature, topography or morphology. To date, almost all field emission measurements from diamond and other wide bandgap materials can be fit with this expression. In many instances, researchers have noted the threshold field for emission. Given the exponential dependence of the emission, there is no true emission threshold, but the value is still useful for comparison, particularly if the threshold emission current is specified.

The moving probe is particularly useful for gaining some insight into where the applied field is concentrated. For emission from typical metal surfaces, if the distance is decreased by any factor, then the emission should be observed at voltages decreased by the same factor. In this case, we can

represent the average field at the surface as the applied voltage divided by the distance (in these studies units of $V/\mu\text{m}$ are often used).

One example where this effect would not hold has been reported by Geis et al. [9] for field emission from nitrogen doped diamond crystals. In this case, it was suggested that the field was applied at the metal–diamond interface (as opposed to the diamond–vacuum interface). The applied field then changes the width of depletion region in the diamond, and there should be little potential drop between the emitting surface to the anode. For this case, the I – V curves would not depend on the average field but would look nearly identical for a wide range of anode to surface distances. The experiments of Geis et al. on type Ib diamond support this model [8]. In this case, the applied field was suggested to assist in supplying the electrons to the diamond conduction band, and the diamond surface was suggested to not affect the emission process.

One of the difficulties of field emission measurements is to determine the anode to sample separation. Initially, we employed a procedure of moving the probe to a condition of touching the surface. We noticed, however, poor reproducibility and occasional damage to the sample and anode. Next, we obtained measurements at each step until the I – V measurements indicated ohmic behavior suggesting that the anode was in contact with the surface. We again found poor reproducibility and occasional damage. Finally, we have employed a procedure in which we record I – V curves for about 20 distances as the probe approaches (but does not touch) the surface. The voltage for a set emission (typically 10 or 100 nA) is plotted vs. relative distance. A straight line was observed in each instance, and the slope of the curve is assigned as the average field. This procedure, which never involves touching, has proven very repeatable and consistent.

Researchers have now recognized other difficulties in measurement of field emission from flat surfaces [10]. One common problem is related to effects due to the emitted electrons striking the anode. If high voltages are employed the electrons strike the anode with sufficient energy to sputter atoms from the surface that may then deposit onto the surface of interest. Moreover, the electrons may desorb enough molecules at the surface to increase the pressure to

the point that an arc or local plasma may occur. These effects often substantially damage the surface, but they often, if not usually, lead to a reduction in the field emission threshold. In the experiments described here, we have limited the maximum applied voltage to less than 1000 V, and the emission current to less than 1 μ A. Even with these limitations, surface damage effects were occasionally observed. The surface damage effects were detected most often with thin diamond films that exhibited relatively high field emission thresholds.

In the experiments described here, a multi-chamber system was employed with a linear UHV sample transfer mechanism. The UHV sample transfer chamber is \sim 14 m long and interconnects 10 different analysis and surface processing chambers. These include UV photoemission, moving probe field emission, III-nitride gas source MBE, surface plasma treatments, metal film deposition and LEED and AES. The system has been described in more detail elsewhere [6].

3. Results and discussion

3.1. NEA surfaces

Prior studies have established the importance of controlling the surface termination to obtain a negative electron affinity [11,12]. The initial studies of diamond deduced that hydrogen termination was necessary to obtain a NEA on the (111) surface. Much later with UV photoemission measurements, it was found that H termination on (100), (110) and (311) surfaces also resulted in a NEA [6,13]. In contrast for surfaces with oxygen termination, an electron affinity of \sim 1.5 eV was detected. For adsorbate free surfaces, the electron affinity was found to be \sim 0.6 eV on the (100) surface. The results for the (100) and (110) surfaces are summarized in Table 1. It is interesting to note that oxygen bonds most strongly on the (100) surface, and this may have been the reason for the long delay in the discovery of the NEA from this surface.

Theoretical analysis confirmed the experimental trends [14]. However, it is impossible to use UV photoemission to measure the position of the vacuum level for a NEA surfaces. Here theory indicated that

Table 1

The UPS spectral width for different diamond (100) and (110) surface terminations

Surface	UPS spectral width (eV)	Electron affinity (eV)
C(100):H	15.7	NEA
C(100) (clean)	15.05	0.65
C(100):O	14.2	1.50
C(110):H	15.7	NEA
C(110) (clean)	15.1	0.60
C(110):O	14.3	1.40

The electron affinity or presence of a NEA is deduced using Eq. (1).

the electron affinity for H terminated surfaces ranges from -2.0 to -3.3 eV depending on the saturation coverage.

The basic picture that develops to explain the role of the surface termination is that the adsorbed layer changes the surface dipole of the material. In the most simple sense, this can be modeled as if the surface dipole layer is a thin capacitor. The potential difference would represent the shift in the vacuum level. The full theoretical calculations demonstrate the magnitude of the effect in noting the \sim 4 eV change in electron affinity from the adsorbate free surface to the H saturated surface [14].

For many years, it has been known that coating semiconductors such as GaAs with low work function metals such as Cs could result in a surface suitable for a cathode for photomultipliers. In fact, these surfaces may have been the first in which the term negative electron affinity was applied. It has been found that Cs and Cs oxide on p-type diamond may also result in a NEA [15]. With the very wide bandgap of diamond, it was supposed that metals with more moderate work functions could be employed, and indeed it was found that titanium with a work function of 4.3 eV resulted in a NEA for thin deposition on diamond (111) surfaces [16]. The picture employed to explain this effect is summarized in Fig. 1. In the model, it is assumed that even for the very thin metal layers employed here, the properties could be modeled in terms of two interfaces: the vacuum–metal interface, and the metal–semiconductor interface. The vacuum–metal interface is described in terms of the metal work function while the metal–diamond interface is described in terms of the Schottky barrier. We note that the metal work func-

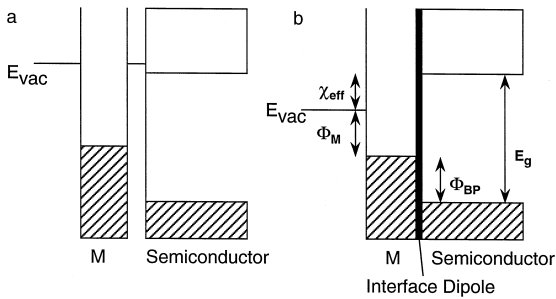


Fig. 1. Schematic of the band alignment with the vacuum level for a thin metal–semiconductor interface for two models. In (a), the metal–semiconductor interface is determined by the Schottky–Mott or work function–electron affinity model. In (b), the Fermi level is pinned in the gap indicating the presence of an interface dipole. Also shown are the effective electron affinity (χ_{eff}), the metal work function (Φ_M), the p-type Schottky barrier (Φ_{BP}), and the band gap (E_g), which display the relationship of Eq. (3).

tion relates the band alignment of the metal and the vacuum, while the Schottky barrier will describe the band alignment of the metal and the semiconductor.

The basic principle for emission through a metal-coated semiconductor is that electrons in the semiconductor may be transported through the metal without scattering. If the vacuum level is below the conduction band minimum of the semiconductor at the metal interface, then the electrons may be emitted into vacuum. This situation may be termed an effective negative electron affinity.

Note that the effect will be determined by the Schottky barrier and the semiconductor electron affinity. Consider first the Schottky–Mott model of a metal semiconductor interface. The relative band alignment is determined by the metal work function and the semiconductor electron affinity (Fig. 1a). Note that in this case, the relationship of the vacuum level to the conduction band minimum of the semiconductor is unchanged by the metal layer. This effect is independent of the metal employed. If the semiconductor exhibits a positive electron affinity prior to metal overcoating, this condition should persist after metal deposition. Similarly, if the semiconductor surface exhibits a NEA prior to metal layer deposition, the Schottky–Mott model would predict the same after metal deposition. Of course, the Schottky barrier at the metal–semiconductor interface would vary linearly with the work function of the metal employed.

For many systems, it is found that the Schottky–Mott model does not apply, and the Schottky barrier is nearly independent of the metal work function. In this case, a low work function metal could be particularly important to induce an effective NEA on diamond [17]. The effective electron affinity (χ_{eff}) would be given in terms of the metal work function (Φ_M) the measured Schottky barrier (here we use the p-type SB, Φ_{BP}) and the band gap, E_g . The relation is given by:

$$\chi_{\text{eff}} = E_g - (\Phi_M + \Phi_{\text{BP}}) \quad (3)$$

The relationship of these variables are shown in Fig. 1b. In addition, prior studies have suggested that the barrier height is also dependent on the termination of the diamond prior to the metal deposition [6]. We note that this model assumes that the thin metal layer can be described by the ‘bulk’ work function and Schottky barrier.

The photoemission results for a series of thin metal layers on O terminated, H terminated and adsorbate free diamond are summarized in Fig. 2. The Schottky barrier heights (determined from the photoemission) of the different metal–diamond interfaces are plotted vs. the metal work function for Zr, Ti, Cu, Co and Ni [17]. The presence of a NEA is indicated by the open and filled data points. The dashed line represents the limiting value of the Schottky barrier for which a NEA is expected for

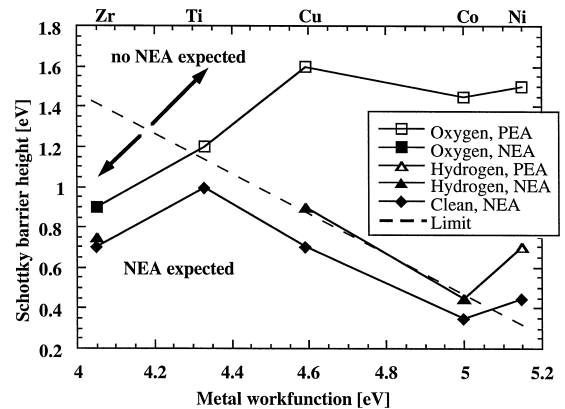


Fig. 2. Summary of photoemission measurements for metal films deposited on p-type diamond. The data indicate the measured Schottky barrier for the different diamond surface termination and metal, and the open points indicate a positive electron affinity while the filled data points indicate a NEA.

metal–diamond interfaces according to Eq. (1) (i.e., setting $\chi_{\text{eff}} = 0$, and using $E_g = 5.45$ eV). Thus, a NEA is expected for data points on or below this dashed line and a positive electron affinity for those above. As is evident, the experimental results for the electron affinity largely agree with this model. One exception is Ni [6]. Based on theoretical studies, it has been suggested that the measured NEA on the Ni covered surface may be indicative of the presence of two configurations of Ni on the surface with different Schottky barrier heights of 0.1 eV and 0.8 eV, respectively. The model would predict that the regions with a Schottky barrier of 0.1 eV would exhibit a NEA while the other regions would exhibit a positive electron affinity.

The results also show that metals deposited on hydrogen terminated and adsorbate free surfaces exhibit a similar dependence except that the Schottky barrier is slightly larger for the H terminated surfaces. In contrast, The Schottky barrier for metals on oxygen terminated diamond is nearly constant except for Ti and Zr. These last two metals are highly reactive, and it is proposed that they displace the oxygen from the metal diamond interface to react directly with the diamond.

We note that the effects of the adsorbate covered surface were described in terms of the change of the surface dipole. In essence, the model described for the metal–diamond interface involves the same effect. The Schottky–Mott model is based on the premise that the interface bonding does not affect the surface dipole of the metal or the semiconductor. In contrast, if the SB is pinned due to defects or other effects, an interface dipole forms, and this interface dipole then accounts for the change in the relative band alignment of the conduction band minimum and the vacuum level.

For the AlN and AlGa_xN alloys, photoemission results have indicated a negative electron affinity for AlN films and AlN rich AlGa_xN alloys [4,5]. In all instances, the films were epitaxial layers grown on the Si surface of 6H–SiC. The photoemission results have indicated a NEA for AlN and a positive electron affinity of 3.3 eV for GaN. The results indicate a NEA for Al_xGa_{1-x}N alloys with $x > 0.65$. The presumed bonding arrangement at the nitride–SiC interface is N bonding to Si of the SiC. Thus, it may be suggested that the NEA surface is the (0001) Al

Table 2

The calculated results of electron affinities (in eV) for different surface configurations

Surface specie	Bare surface	H-terminated (1×1)	Vacancy (2×2)
Diamond(111)	positive	-1.5	N.A.
Al–AlN	+0.85	+1.60	-0.70
N–AlN	+0.30	+0.05	+1.40

surface of the AlN. Moreover, little is known of the effects of various surface terminations on the nitride surfaces. Some insight may be gained from theoretical studies which have compared the hexagonal (111) surface of diamond to AlN [18]. The results are summarized in Table 2. Here it may be suggested that the NEA surface is actually a 2×2 reconstruction with vacancies for charge equilibrium. It is also apparently possible to obtain a NEA for the H-terminated N surface of AlN.

3.2. Field emission

The field emission measurements of NEA p-type diamond single crystal and thin film AlN on 6H–SiC exhibit similar characteristics. Both materials exhibit field emission thresholds (at ~ 100 nA) of ~ 25 V/ μm [12,18].

We have extensively studied the properties of field emission from p-type diamond crystals with various surface treatments [13]. The goal of the study is to determine if the field emission threshold is related to the NEA properties. A typical set of I – V traces for different probe distances are shown in Fig. 3. In these measurements, the I – V curves exhibit similar characteristics if the V is normalized by the distance. As noted above, this indicates that the emission is limited by a tunneling process. A likely possibility is that the electrons tunnel through a barrier at the surface of the p-type diamond. The I – V curves were analyzed to obtain an average field for threshold emission. For this case, we considered the threshold emission as an emission current of 0.1 μA . The results for different diamond surfaces are indicated in Table 3. It is evident that surfaces that exhibit a lower or negative electron affinity also exhibited a lower field emission threshold. These results demonstrate a clear correlation between the

field emission and the properties of the surface for emission from p-type diamond.

Prior photo and field emission studies of p-type diamond have suggested that the field emission results from electrons in the valence band while the photoemission is due to electrons emitted from the conduction band. The results presented here are also consistent with this model. If the emission is from the valence band, then lowering the electron affinity will lower the barrier for emission. A negative electron affinity will still result in a barrier to emission albeit lower than for a surface that exhibits a positive electron affinity. The fact that the emission is described by the F–N equation also supports this model.

While field emission is a more complicated process that involves carrier supply, transport to the surface and emission, for the p-type diamond, it is apparently only limited by the emission. Given that so many studies have highlighted the effects due to the supply contact, how is there a difference here? The answer is that the carriers in the diamond are actually holes migrating toward the supply contact. The small Schottky barrier to holes provides a negligible resistance as does the transport. We note that emission from nitrogen doped or n-type diamond should have substantially different properties. Here it is likely that the major barrier to emission is at the metal–diamond interface.

We have not carried out such extensive experiments on the AlN/SiC system, but we may suggest some similarities and differences. The I – V curves are fit by the F–N expression and they scale with the

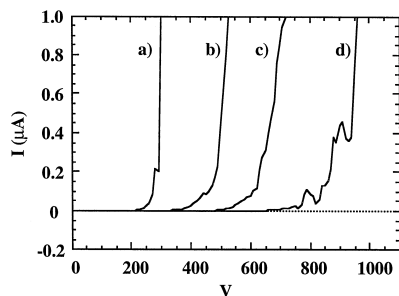


Fig. 3. Field emission current–voltage curves for Zr on a oxygen terminated type IIb single crystal diamond (100) sample. Approximate distances between the sample and the anode: (a) $5.7 \mu\text{m}$, (b) $9.7 \mu\text{m}$, (c) $12.4 \mu\text{m}$, (d) $17.2 \mu\text{m}$. The distances were obtained from contact of the anode and the surface.

Table 3

Results comparing UV photoemission and electron field emission measurements

Sample	UPS	Field emission threshold ($\text{V}/\mu\text{m}$)
C(100) oxygen	PEA, $\chi \cong 1.4 \text{ eV}$	79
C(110) oxygen	PEA, $\chi \cong 0.6 \text{ eV}$	81
C(110) hydrogen	NEA, $\chi < 0$	25
Co/C(100) clean	NEA, $\chi < 0$, $\Phi_{\text{B}} \cong 0.35 \text{ eV}$	30
Co/C(100) hydrogen	NEA, $\chi < 0$, $\Phi_{\text{B}} \cong 0.45 \text{ eV}$	39
Co/C(100) oxygen	PEA, $\chi \cong 0.75 \text{ eV}$, $\Phi_{\text{B}} \cong 1.40 \text{ eV}$	52

PEA: positive electron affinity; NEA: negative electron affinity. The field emission average field to obtain a current $0.1 \mu\text{A}$ is indicated.

probe to anode distance. Thus, there is no depletion region in the AlN to affect the field vs. distance. Here it seems likely that the barrier to emission is the SiC–AlN interface. The electrons tunnel through this barrier with F–N type characteristics. The assumption is that the AlN is undoped and behaves as a simple dielectric. The field at the SiC–AlN interface will then be linearly proportional to the average field determined by the applied voltage divided by the anode to sample distance. Our prior studies have suggested that the conduction band offset between AlN and 6H–SiC is 2.4 eV , which could be similar to the barrier at a NEA diamond surface. For SiC, we have shown that the electron affinity is $\sim 3.3 \text{ eV}$. Thus, even if the AlN behaves as a simple dielectric, the barrier to emission would be reduced for AlN on SiC as compared to an uncoated surface.

3.3. PEEM and FEEM of nitride emitter arrays

The research field of vacuum emitters has focused on metallic structures with sharp tips to obtain field enhancement. The field enhancement is related to the radius of curvature of the pointed structure and to the height above the base. Recently, selective growth process have been demonstrated for GaN [19]. The

most unique aspect of the growth process is that the preference for a low energy surface leads to the growth of essentially perfect hexagonal pyramidal structures. The growth involves a mask of SiO_2 on a (0001) GaN film. Circular holes are etched in the oxide to expose the underlying GaN. When the film is returned into the OMVPE growth system, the growth proceeds only on the exposed GaN areas, and pyramids develop with the (1–101) surfaces exposed. A SEM micrograph of the surface is shown in Fig. 4.

Field emission from these surfaces using the moving probe system indicated field emission thresholds at fields as low as $7 \text{ V}/\mu\text{m}$ (for an emission current threshold of 10 nA). The curves could be fit with the Fowler–Nordheim expression. Moreover, the I – V curves scaled with the distance indicating again that the same average field was required for different distances from the probe. As noted above this suggests that the emission is limited by the exposed surface. Given that the electron affinity of GaN has been measured to be 3.4 eV, it is evident that the emission is enhanced by the structure of the pyramids, presumably due to field enhancement.

To examine the location of the emission, we initiated measurements employing a UV photo-electron emission microscope (PEEM). The system involves UV light to cause photoelectron emission from the surface. The sample sits at the focal point

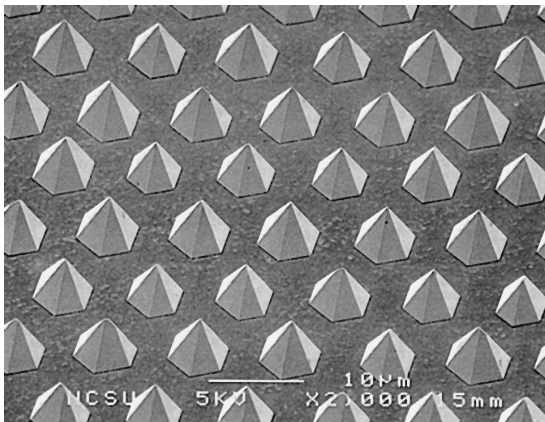


Fig. 4. A SEM image of the pyramidal n-type GaN (Si doped) tips prepared by selective growth of GaN through an oxide mask with $\sim 1 \mu\text{m}$ circular holes. The spacing between the pyramidal tips is $10 \mu\text{m}$.

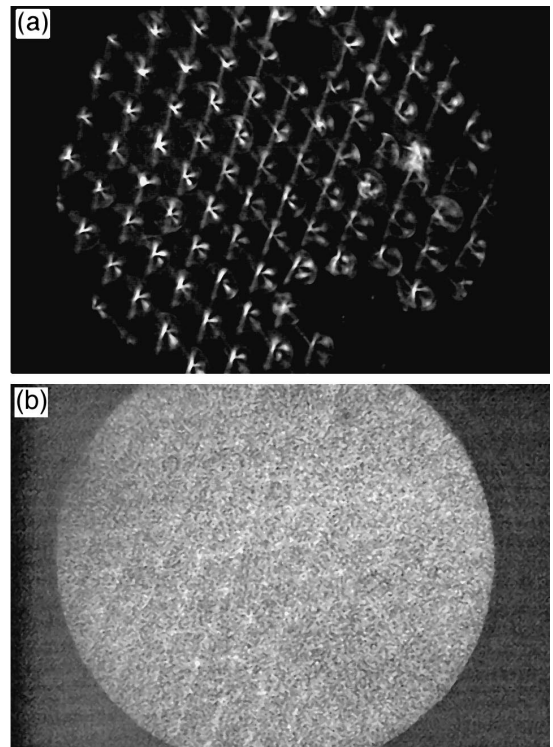


Fig. 5. PEEM (a) (photo-electron emission microscopy) and FEEM (b) (field electron emission microscopy) images of an array of Si doped GaN pyramidal peaks. The images were obtained in the same microscope with the UV light on for the PEEM and no photo-excitation in the FEEM. Both images were obtained with an accelerating voltage of 20 kV applied over $\sim 2 \text{ mm}$ at the sample. The field of view in (a) and (b) is $150 \mu\text{m}$.

of a multi element electron optics system that images the electrons onto a microchannel plate, and the image is recorded with a CCD video camera. The microscope has a demonstrated resolution of 12 nm. The electrons are accelerated to 20 kV in the imaging system. In the Elmitec microscope, the sample is at ground potential. The 20 kV results in a field of $10 \text{ V}/\mu\text{m}$. While field emission is not detected from typical samples at this field, the low field emission threshold of the GaN pyramid array will allow FEEM (field electron emission microscopy) to detect the source of emission.

Shown in Fig. 5 is a PEEM and FEEM image of the same GaN emitter array. Note that the emission is concentrated at the points of the emitter arrays in both images. The PEEM images show an asymmetry

of the edges apparently due to shadowing of the UV light (it is incident at an average angle of 84° from normal). The emission appears relatively uniform over the emitter array. It is evident that the emitter arrays offer the possibility of enhanced emission at relatively low fields, and the emission may be more controlled than from flat surfaces.

We note that emitter structures based on flat epitaxial films of AlN and graded GaN–AlGaIn (on n-type 6H–SiC) film structures have been fabricated, and these structures demonstrated emission at relatively low applied voltages of 40 V [20]. It would appear that similar structures fabricated with the emitter arrays could achieve emission at even lower applied voltage.

4. Summary and conclusions

The results presented here indicate that NEA surfaces may be obtained for diamond and other wide bandgap nitride materials. For adsorbate covered surfaces, the effect can be related to the change of the surface dipole due to the bonding of the adsorbate layer. In general, if the adsorbate is more electronegative than the substrate, then the adsorbate will increase the electron affinity while the opposite will occur if the adsorbate is more electropositive. For thin metal layers, the occurrence of an effective NEA can be understood in terms of the Schottky barrier and metal work function. The experimental results indicate NEA behavior for metals such as Ti or Zr which can displace interface oxygen, and exhibit relatively low work function values.

The field emission results for p-type diamond indicate that the threshold field is lowered for a NEA surface. However, Fowler–Nordheim characteristics are still observed, suggesting a tunneling process at the surface. The results are consistent with the model that the electrons originate from the valence band of the diamond for p-type diamond.

In contrast, for AlN epitaxial films on n-type 6H–SiC, it appears that the emission originates from the conduction band of the SiC and the AlN behaves as a simple dielectric but with a NEA so that there is no surface charging.

PEEM and FEEM images of Si doped GaN pyramid structures were reported. The structures dis-

played field emission at an average field of ~ 10 V/ μm . The FEEM images demonstrated that the emission originated largely from the points and edges of the pyramid structures. Thus, field enhancement plays a significant role in the emission. Because the material is known to be n-type, it may be presumed that the emission originates from electrons in the conduction band. Both the PEEM and FEEM images displayed nearly uniform emission from many emitter tips.

Acknowledgements

We gratefully acknowledge the support of the Office of Naval Research.

References

- [1] F.J. Himpsel, J.A. Knapp, J.A. van Vechten, D.E. Eastman, *Phys. Rev. B* 20 (1979) 624.
- [2] B.B. Pate, *Surf. Sci.* 165 (1986) 83.
- [3] M.J. Powers, M.C. Benjamin, L.M. Porter, R.J. Nemanich, R.F. Davis, J.J. Cuomo, G.L. Doll, S.J. Harris, *Appl. Phys. Lett.* 67 (1995) 3912.
- [4] M.C. Benjamin, C. Wang, R.F. Davis, R.J. Nemanich, *Appl. Phys. Lett.* 64 (1994) 3288.
- [5] M.C. Benjamin, M.D. Bremser, T.W. Weeks Jr., S.W. King, R.F. Davis, R.J. Nemanich, *Appl. Surf. Sci.* 104/105 (1996) 455.
- [6] J. van der Weide, R.J. Nemanich, *Phys. Rev. B* 49 (1994) 13629.
- [7] C. Bandis, B.B. Pate, *Phys. Rev. Lett.* 74 (1995) 777.
- [8] R. Gomer, *Field Emission and Field Ionization*, Cambridge, MA, 1961.
- [9] M.W. Geis, J.C. Twichell, N.N. Efremow, K. Kohn, T.M. Lyszczarz, *Appl. Phys. Lett.* 68 (1996) 2294.
- [10] O.M. Kuttel, O. Groning, E. Schaller, L. Diedrich, P. Groning, L. Schlapbach, *Diamond Related Mater.* 5 (1996) 807.
- [11] R.J. Nemanich, P.K. Baumann, M.C. Benjamin, S.P. Bozeman, B.L. Ward, *Proceedings of the Int. School Physics Enrico Fermi*, IOS Press, Amsterdam, 1977, p. 537.
- [12] R.J. Nemanich, P.K. Baumann, M.C. Benjamin, S.W. King, J. van der Weide, R.F. Davis, *Diamond Related Mater.* 5 (1996) 790–796.
- [13] P.K. Baumann, R.J. Nemanich, *Surf. Sci.*, in press.
- [14] Z. Zhang, M. Wensell, J. Bernholc, *Phys. Rev. B* 51 (1995) 5291.
- [15] M.W. Geis, J.C. Twichell, J. Macaulay, K. Okano, *Appl. Phys. Lett.* 67 (1995) 1328.

- [16] J. van der Weide, R.J. Nemanich, *J. Vac. Sci. Technol. B* 10 (1992) 1940.
- [17] P.K. Baumann, R.J. Nemanich, *J. Appl. Phys.* 83 (1998) 2072.
- [18] R.J. Nemanich, M.C. Benjamin, S.W. King, M.D. Bremser, R.F. Davis, B. Chen, Z. Zhang, J. Bernholc, in: F.A. Ponce, R.D. Dupuis, S. Nakamura, J.A. Edmond (Eds.), *Gallium Nitride and Related Materials*, Mater. Resl. Soc. Symp. Proc. 395, Boston, MA, Fall 1995, pp. 777–788.
- [19] O.-H. Nam, M.D. Bremser, B.L. Ward, R.J. Nemanich, R.F. Davis, *Jpn. J. Appl. Phys.* 36 (1997) L532.
- [20] A.T. Sowers, J.A. Christman, M.D. Bremser, B.L. Ward, R.F. Davis, R.J. Nemanich, *Appl. Phys. Lett.* 71 (1997) 2289.